Moroccan Journal of Chemistry
ISSN: 2351-812X
http://revues.imist.ma/?journal=morjchem&page=login
Kaddouri & al. / Mor. J. Chem. 5 N°3 (2017) 467-475

Two tripodal pyrazolic ligands: application against corrosion of mild steel in HCl 1M

Y. Kaddouri[(a)*], A. Takfaoui[(a)], M. Lamsayah[(a)], M. El Azzouzi[(b)], R. Boyaala[(a)], A. Chetouani[(b)], A. Zarrouk[(b)], B. Hammouti[(b)], R. Touzani[(a,c)]

[(a)]Laboratory of Applied Chemistry and Environment (URAC 18), Faculty of Sciences, University Mohammed Premier, P. O. Box 4808, 60046 Oujda, Morocco

[(b)] Laboratory of Applied Analytical Chemistry, Materials and Environment, Faculty of Sciences, University Mohammed Premier, P. O. Box 4808, 60046 Oujda, Morocco.

[(c)] Multidisciplinary Faculty, BP. 300, Selouane 62 702 Nador, Morocco

Abstract

Two tripodal pyrazolic ligands: N,N-bis((3,5-diméthyl-1H-pyrazol-1-yl)methy)-2,4-difluoroaniline (**2Fpyr 1**) and N,N-bis((1H-pyrazol-1-yl)methyl)-2,4-difluoroaniline (**2Fpyr 2**) were synthetized in good yiels. Then we applied them against corrosion of mild steel in HCl 1M solution. Weight loss measurement give us the inhibition efficiencies values reached 80.2 % for **2Fpyr1** and 77.3 % for **2Fpyr 2** at the concentration 10^{-3}, then by changing the temperature from 313K to 343 K, which give us the activation and adsorption parameters, and we reveal from it that the ligands **2Fpyr 1** were adsorbed according to Langmuir Isotherm, but **2Fpyr 2** were was adsorbed according to El-Awady adsorption Isotherm, we obtain these results using certain isotherms as Langmuir, Freundlich, Temkin, Frumkin, Florry-Huggins, Adejo-Ekwenchi and El-Awady. We conclude from polarization curves that all the ligands are mixed type inhibitors (anodic and cathodic type inhibitors), and from the impedance diagrams in the Nyquist presentation which are in the form of one half loop because that the corrosion is controlled by charge transfer process. We used GAUSSIAN 09W program to do theoretical investigations by considering the Density Functional Theory (DFT) method to calculate quantum parameters as E_{HOMO}, E_{LUMO}, ΔE_{HOMO}-E_{LUMO} and μ dipolar moment that allows us to confirm experimental results obtained from gravimetric and electrochemical studies.

** Corresponding author:*
yassine.kaddouri92@gmail.com
Received 10 Feb 2017,
Revised 15June 2017,
Accepted 20 July 2017

Keywords: *Ligand, pyrazole, corrosion, HCl, mild steel, Tafel, EIS, weight loss, adsorption, Langmuir, Freundlich, Temkin, Frumkin, Florry-Huggins, Adejo-Ekwenchi, El Awady, quantum calculations, GAUSSIAN 09W, DFT.*

1. Introduction

Tripodal pyrazolic ligands [1-8] are known one of the most used organic inhibitors of mild steel corrosion, due to the presence of nitrogen in the structure which facilitates the adsorption on the surface of the metal, and forming a thin protective film to decrease the dissolution of the metal [9]. The inhibition efficiency of these molecules in aggressive environment is due to their adsorption on the surface of the metal. This phenomenon could be put in place by electrostatic interaction between (i) the charged metal and the charged inhibitor molecules, (ii) dipolar interactions between non-charged inhibitor molecules and the metal, (iii) the π-interactions with the metal, or the combination of these propositions. Our objective is to study the relation structure-activity (corrosion inhibition) of two tripodal pyrazolic ligands which differenced by the substituents on the pyrazoles, we will experimentally use the weight loss measurements and Polarization measurements, then we will compare it with theoretical results obtained using GAUSSIAN 09W.

2. Materials and methods

2.1. Experimental section

We have synthetized two tripodal pyrazolic ligands (**Figure 1**) as previous described method [10], they are obtained by using two Pyrazole derivatives: (1H-pyrrol-1-yl) methanol and (2,4-dimethyl-1H-pyrrol-1-yl) methanol, then we have test their activity against mild steel corrosion in HCl 1M solution. The ligands have been purified by recrystallization then characterized using FTIR, ^{1}H NMR, ^{13}C NMR spectroscopy and mass spectroscopy analysis.

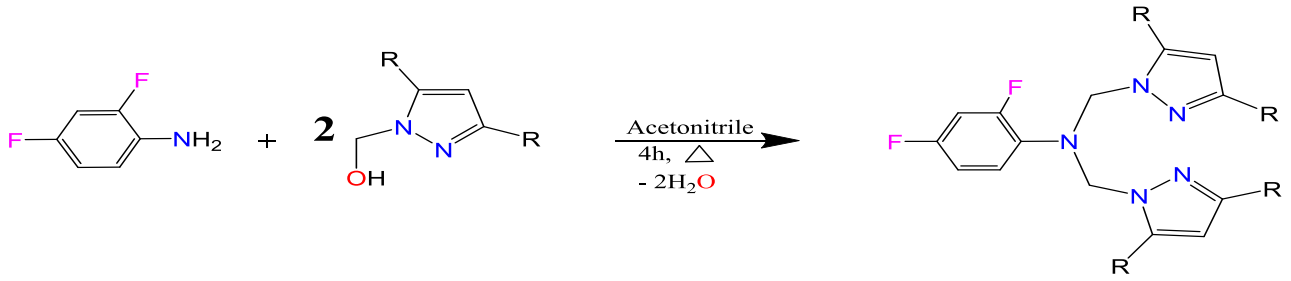

Figure 1. Synthesis of the ligands **2Fpyr 1** et **2Fpyr 2**

For the corrosion experiments, we will use the same methods as previously done [10].

2.2. Computational chemistry

To know which of the two ligands are more efficient than the other one against corrosion of mild steel, we use the GAUSSIAN 09W [11] suite and by the DFT (density functional theory) method while adopting the functional hybrid B3LYP which use the three functional parameters of Becke (B3) and include the mixed exchanged terms of HF and DFT associated to the functional correlation gradient corrected of Lee, Yang and Parr (LYP), and the base is 6-31G (d,p). We reveal the quantum chemistry descriptors as E_{HOMO}, E_{LUMO}, the energy gap ΔE(gap), dipole moment (μ), hardness (η), ionization energy (I), and the number of transferred charges ΔN after optimization of all the geometric variables without any symmetry constraints.

3. Results and Discussions

3.1. Characterization of ligands

NMR spectroscopy, FTIR and Mass spectroscopy of the two ligands have spectral data according to the literature [12].

3.2. Weight loss measurements

3.2.1. The concentration effect

By changing the concentration of the inhibitor in the aggressive solution we obtained the following results in **Table 1**

Table 1. The corrosion rates and inhibitory efficiencies of the **2Fpyr 1** and **2Fpyr 2** at different concentrations in a solution of HCl 1M

	Concentration	**V_{corr} (mg.cm^{-2}.h^{-1})**	**EI (%)**
Blanc	1	0.940	
2Fpyr 1	10^{-3}	0.1861	80.2
	5.10^{-4}	0.2801	70.2
	10^{-4}	0.5132	45.4
	5.10^{-5}	0.7256	22.8
	10^{-5}	0.7755	17.5
2Fpyr 2	10^{-3}	1.8833	79.9
	5.10^{-4}	2.2046	76.6
	10^{-4}	3.9243	58.3
	5.10^{-5}	4.7252	49.8
	10^{-5}	5.3829	42.8

The addition of the inhibitor molecules decreases the corrosion rate with the increase of their concentration, by the table data we can class them as: **2Fpyr 1** (%EI= 80.2 %) > **2Fpyr 2** (%EI= 79.9%)

3.2.2. The temperature effect

By using the concentration which give us the highest inhibition efficiency which is 10^{-3} M, we fix it and we change the range of temperature from 40 °C to 70°C, we obtained the results in the **Table 2**. Generally, the rise of the temperature causes the weakening of the van der waals interactions between the inhibitor and the metal, which conclude the acceleration of corrosion [13]

Table 2. The corrosion rates and inhibitory efficiencies of **2Fpyr 1** and **2Fpyr 2**.

T(K)	**C(M)**	**2Fpyr 1**		**2Fpyr 2**	
		V_{corr} (mg.cm^{-2}.h^{-1})	**EI (%)**	**V_{corr} (mg.cm^{-2}.h^{-1})**	**EI (%)**
313	Blanc	1.775			
	10^{-3}	0.9727	45.2	0.7165	59.6
323	Blanc	3.053			
	10^{-3}	2.0797	31.9	1.7027	44.2
333	Blanc	5.371			
	10^{-3}	4.2447	20.9	3.8662	28.0
343	Blanc	8.336			
	10^{-3}	7.3903	11.3	7.1876	13.8

3.2.3. The activation thermodynamic parameters

Previously, we say that the rise of the temperature causes the desorption of the inhibitor molecules which is very important in our study because of the presence of the fluorine substituents. Several studies [14-16] shows that the evolution of the metal surface covered by the inhibitor molecules causes the decrease of activation energy. Mathematically, we express the corrosion rate which depends on the temperature by the equation of Arrhenius (5)(6) to know the activation energy, and we use the Arrhenius equation of transition [17] (7) to extract the other thermodynamic parameters:

$$\mathbf{V_{corr}} = \mathbf{A}.\mathbf{e}^{-\frac{Ea}{R.T}} \quad (5)$$

from where $$Ln\,(V_{corr}) = \ln A - \frac{Ea}{R.T} \quad (6)$$

$$V_{corr} = \frac{R.T}{N_A.h}.\exp\left(\frac{\Delta Sa^{\circ}}{R}\right).\exp\left(-\frac{\Delta Ha^{\circ}}{R.T}\right) \quad (7)$$

Where in (5) V_{corr} is the corrosion rate (mg/cm².h), E_a: the apparent activation energy (depends on the unit of the constant R), A: Arrhenius pre-exponential parameter, T: the absolute temperature (Kelvin), R: perfect gas constant and K a constant. And for (7) h is Plank constant, N_A : Avogadro number, ΔHa°: the enthalpy of activation and ΔSa°: the entropy of activation.

Table 3. The thermodynamic parameters values of activation for mild steel in molar hydrochloric acid in the absence and the presence of **2Fpyr 1** and **2Fpyr 2**.

	C (M)	Ea (kJ/mol)	ΔH_a° (kJ/mol)	ΔS_a° (kJ/mol.K)	$Ea-\Delta H_a^{\circ}$ (kJ/mol)
	Blanc	46.49	43.77	-100.60	2.72
2Fpyr 1	10^{-3}	60.74	58.02	-59.88	2.72
2Fpyr 2	10^{-3}	69.15	66.43	-35.52	2.72

By the ranking of Radovici [17] the Energy of activation in the Table 3 of the inhibitor are higher than without them. That could be attributed to the adsorption of the inhibitor molecules on the surface of the metal which decrease the interactions between the metal and the environment. The values of ΔH_a° are positive, that reflect the endothermic nature of the metal dissolution process, also blocked because their values in the case of inhibitors presence are higher than without them. The energy of activation values is bigger than ΔH_a° which indicate that the corrosion process involves the formation of H_2.

3.2.4. The adsorption isotherm

To know the adsorption isotherm, we go to evaluate many adsorption isotherms described in the literature [18-24]. Generally, the adsorption isotherm links the surface coverage (θ) (8) with the inhibitor concentration C_{inh}.

$$\theta = \frac{V_{corr} - V_{corr\,(inh)}}{V_{corr}} \quad (8)$$

To find the corresponding adsorption isotherm of **2Fpyr 1** and **2Fpyr 2**, we compare the correlation coefficients (R^2) that are assembling in the Table 4

Table 4. The correlation coefficient R^2 values obtained for each isotherm and for **2Fpyr 1** and **2Fpyr 2**.

	Langmuir	Freundlich	Temkin	Florry-Huggins	Frumkin	Adejo-Ekwenchi	El-Awady
2Fpyr 1	0.9865	0.9398	0.9394	0.8461	0.4855	0.9081	0.9496
2Fpyr 2	0.8283	0.9266	0.915	0.3927	0.4755	0.986	0.9885

By the previous data, we conclude that **2Fpyr 1** obey the Langmuir adsorption isotherm, and **2Fpyr 2** obey the El-Awady adsorption isotherm.

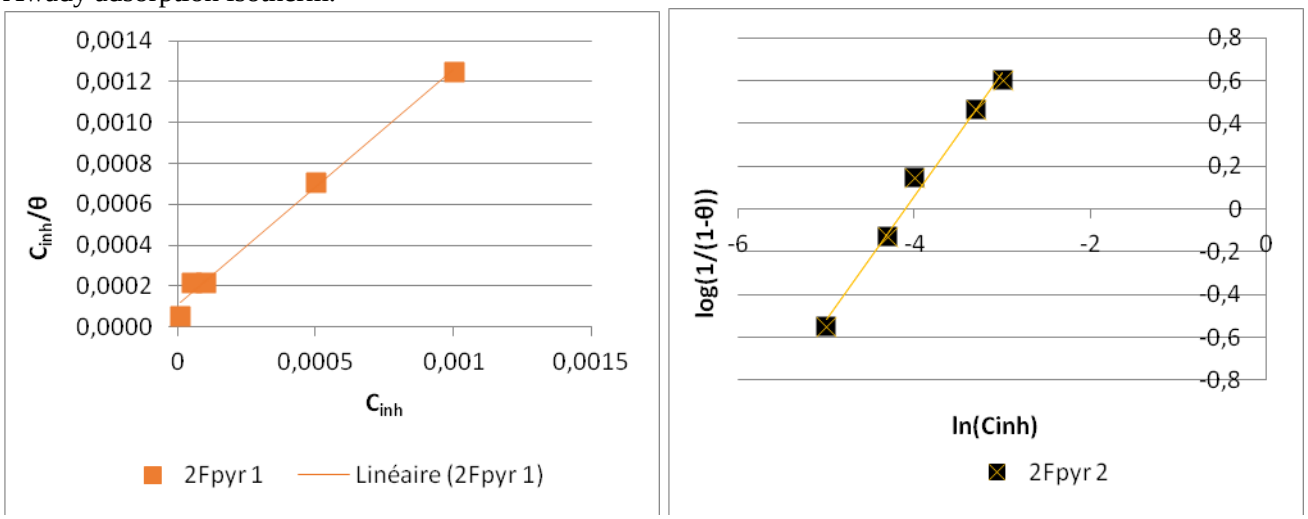

Figure 2. Trace of adsorption isotherm curves for **2Fpyr 1** (left) and **2Fpyr 2** (right).

After that we will calculate the standard adsorption free energy ΔG°_{ads} using the following equation:

$$\Delta G^{\circ}_{ads} = -RTLn(55,5K_{ads}) \quad (9)$$

Where ΔG°_{ads}: the standard adsorption free energy, R: constant of the perfect gas, T: The absolute temperature in Kelvin (K), 55,5 the concentration of water in solution in mol/dm3, K_{ads} : Equilibrium constant for adsorption process. Because of the higher value of K_{ads} for **2Fpyr 1** there is strong interactions between their molecules and the metal surface. And from the values of ΔG°_{ads} which in the range [-20kJ/mol, -40kJ/mol] so they are physisorbed and chemisorbed, also because of their negativity their reaction is spontaneous and that **2Fpyr 1** form a monolayer on the metal surface but a multilayer for **2Fpyr 2** (the value of b in the linear form is 1.73 so the molecules of **2Fpyr 2** occupies more than one active site on the metal surface).

Table 5. The thermodynamic parameters of **2Fpyr 1** and **2Fpyr 2**.

	Adsorption isotherm	K_{ads}	ΔG°_{ads}(kJ/mol)
2Fpyr 1	Langmuir	6630.42	-32.82
2Fpyr 2	El-Awady	235.9	-24.28

3.3. Polarization measurements

3.3.1. Potentiodynamic polarization

From the table 6 data, we note that the addition of inhibitor into the solution causes the decrease of the corrosion current density and also the slopes of Tafel βc and βa. From the curves, we see that the cathodic curves present linearity which indicate that reaction of the reduction of H_2 on the metal is made according to pure activation mechanism. For an overvoltage, more than -300mV/ECS appear on the curves as overlapped on the blank one, suggesting the inhibitor desorption and therefore the dissolution dominates the anodic reaction. The marked decrease of the cathodic current density and in more negative potentials than -300mV/ECS, in the anodic range, plus the slight

shift of the free potential towards the lower noble values, shows that studied inhibitors are mixed type with a cathodic predominance. The inhibitory efficacy of the tested compounds increases the following order:

L4 (%IE= 84,43%) > L2 (%IE= 80,78%)

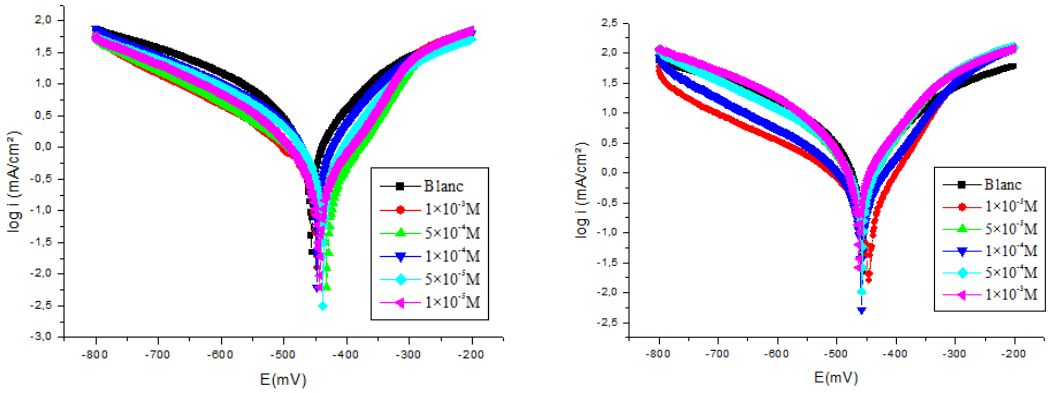

Figure 3. The polarization curves of mild steel in HCl without and with addition of different concentrations of **2Fpyr 1** (left) and **2Fpyr 2** (right).

Table 6. The electrochemical parameters and inhibition efficiency of the corrosion of mild steel in HCl 1M for different concentrations for **2Fpyr 1** and **2Fpyr 2**.

	C(M)	E_{corr} (mV/SCE)	β_c (mV/dec)	β_a (mV/dec)	Icorr(µA/cm²)	EI (%)
Blanc	1	-457.3	-218	172.5	3280.8	
2Fpyr 1	1.10^{-3}	-464.9	-198.6	75.2	510.7	84.43
	5.10^{-4}	-464.2	-206.9	82.7	775.7	76.36
	1.10^{-4}	-463.8	-87.1	78.9	863.7	73.67
	5.10^{-5}	-462.5	-211.3	94.1	971.1	70.40
	1.10^{-5}	-463.4	-223.9	98.3	1274.5	61.15
2Fpyr 2	1.10^{-3}	-431.6	-184.2	91.2	630.7	80.78
	5.10^{-4}	-448.4	-197.6	100	779.8	76.23
	1.10^{-4}	-444.3	-180.6	104.9	911.2	72.23
	5.10^{-5}	-438.7	-191.3	122.2	1301.3	60.34
	1.10^{-5}	-449	-194.5	128.5	1684.5	48.65

3.3.2. Electrochemical impedance spectroscopy (EIS)

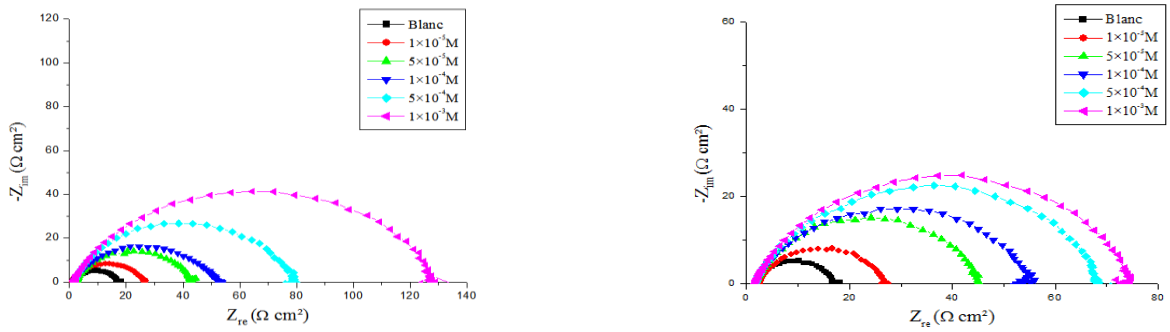

Figure 4. The impedance diagrams for **2Fpyr 1** (left) and **2Fpyr 2** (right).

We see in **Figure 4** that all the EIS diagrams are constituted of one half loop, what it means that the reaction of the inhibitors **2Fpyr 1** and **2Fpyr 2** is controlled by charge transfer process on a solid electrode that have a heterogeneous and irregular surface. All the parameters are collected in **Table 7**.

Table 7. The electrochemical parameters and inhibition efficiency of mild steel in 1M HCl in the presence of **2Fpyr 1** and **2Fpyr 2** at various concentrations obtained E_{corr} (T=35°C).

	C(M)	R_Ω (Ω.cm²)	R_t (Ω.cm²)	F_{max} (Hz)	C_{dl} (µF/cm²)	IE (%)
Blanc	1	1.996	14.994	63.29	167.79	
2Fpyr 1	1.10^{-3}	1.163	129.24	20	61.60	88.39
	5.10^{-4}	1.444	77.20	25	82.5	80.58
	1.10^{-4}	1.565	47.25	40	84.24	68.27
	5.10^{-5}	2.2	40.63	31.64	123.17	63.09
	1.10^{-5}	2.074	25.82	50	123.34	41.93
2Fpyr 2	1.10^{-3}	1.489	74.07	15.82	92.55	79.76
	5.10^{-4}	1.623	54.38	31.64	95.51	77.96
	1.10^{-4}	1.46	52.69	31.64	109.06	72.43
	5.10^{-5}	1.494	46.14	31.64	130.91	67.50
	1.10^{-5}	2.593	24.33	50	135.9	38.36

First of all, we see that **2Fpyr 1** is more efficient against corrosion than **2Fpyr 2** with inhibition efficiency respectively 88,39% and 79,76% in 10^{-3}M, which is related to the increase of R_t as the concentration of inhibitor increase, but the double layer capacity (C_{dl}) values decrease due to the adsorption of the inhibitor molecules on the surface of the metal, causing the decrease of their active surface.

3.4. Theoretical studies

3.4.1. Density functional theory (DFT) method

3.4.1.1. Structure optimization and quantum parameters

By the use of GAUSSIAN 09W and the density functional theory (DFT) where we consider that the inhibitors are in their isolate state in the B3LYP/6-31 G (d,p). The optimized structure, the HUMO and the LUMO are represented in Figure 5. After optimizing the structure, we calculate the energy to calculate the quantum parameters using the next equations:

$\Delta E(gap) = E_{HOMO} - E_{LUMO}$ (10)

By the Koopmans theory [25] we have:

$I = - E_{HOMO}$ (11)

$A = - E_{LUMO}$ (12)

$\eta = \frac{I-A}{2}$ (13)

By the Pearson scale of electronegativity [26] we calculate the number of electron transferred as:

$$\Delta N = \frac{\chi_{Fe} - \chi_{inh}}{2(\eta_{Fe} - \eta_{inh})} \quad (14)$$

We note from the table data that: **2Fpyr 1** has the highest E_{HOMO} so it's the more donor and **2Fpyr 2** is the more acceptor because of it is highest E_{LUMO} value. **2Fpyr 1** is the easiest molecule that could be excited and it is more reactant than **2Fpyr 2** because of it is highest ionization energy value (I).**2Fpyr 1** is easy to assign electron due to the

lowest value of hardness (η), and it is plus adsorbed because of the highest value of Number of electron transferred (ΔN).

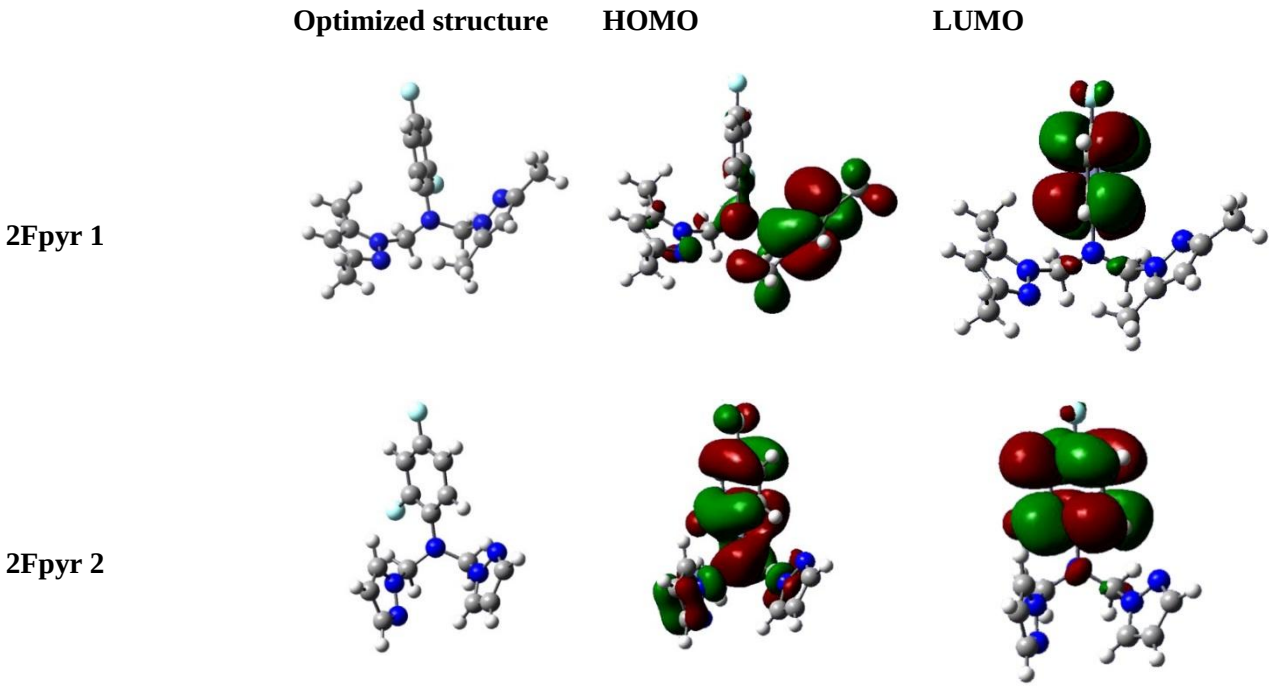

Figure 5. The optimized structures and their HOMO, LUMO representations of **2Fpyr 1** and **2Fpyr 2**.

Table 8. The values of the quantum parameters found and calculated after geometrical optimization using GAUSSIAN 09W.

Quantum parameters	E_{HOMO}	E_{LUMO}	$\Delta E_{(gap)}$	**μ**	**I**	**η**	**ΔN**
2Fpyr 1	-0.22003	-0.01611	0.20392	2.5191	0.22003	0.10196	-0.350840791
2Fpyr 2	-0.22263	-0.01609	0.20654	0.8312	0.22263	0.10327	-0.355281846

4. Conclusion

We conclude that **2Fpyr 1** is the best inhibitor, it gives an inhibition efficiency of 80.2% by weight loss measurements, obey the Langmuir adsorption isotherm because of the presence of methyl substituents which covers the electro attractors effect of the fluorine on the benzene, it forms a monolayer on the surface of the metal. From the polarization curves, we see that **2Fpyr 1** with inhibition efficiency equal to 84.43% and it is mixed type inhibitors with a cathodic predominance. For the EIS diagrams which are constituted of one half loop, what it means that the reaction of the inhibitors **2Fpyr 1** and **2Fpyr 2** is controlled by charge transfer process on a solid electrode that have a heterogeneous and irregular surface, they show that **2Fpyr 1** is more efficient against corrosion with a value of 88.4 %. About the theoretical investigations, they are well correlated with the experimental results.

References

[1] S. El Arrouji, K. Ismaily Alaoui, A. Zerrouki, S. EL Kadiri, R. Touzani, Z. Rais, M. Filali Baba, M. Taleb, A. Chetouani, A. Aouniti, *J. Mater. Environ. Sci.* 7 (1) (2016) 299-309.

[2] Y. ELouadi, F. Abrigach, A. Bouyanzer, R. Touzani, O. Riant, B. ElMahi, A. El Assyry, S. Radi, A. Zarrouk, B. Hammouti, *Der Pharma Chemica*, 7 (8) (2015) 265-275.

[3] K. Ismaily Alaoui, F. El Hajjaji, M. A. Azaroual, M. Taleb, A. Chetouani, B. Hammouti, F. Abrigach, M. Khoutoul, Y. Abboud, A. Aouniti, R. Touzani, *J. Chem. Pharm. Research, 6 (7) (2014) 63-81.*

[4] H. Zarrok, A. Zarrouk, R. Salghi, M. Assouag, N. Bouroumane, E.E. Ebenso, B. Hammouti, R. Touzani, H. Oudda, *Der Pharmacia Lettre*, 5 (3) (2013) 327-335.

[5] H. Bendaha, A. Zerrouk , A. Aouniti, B. Hammouti, S. El Kadiri, R. Salghi, R. Touzani, *Phys. Chem. News 64 (2012) 95-103.*

[6] A. Zarrouk, H. Zarrok, R. Salghi, N. Bouroumane, B. Hammouti, S. S. Al-Deyab, R. Touzani , *Int. J. Electrochem. Sci.*, 7 (2012) 10215-10232.

[7] B. Zerga, A. Attayibat, M. Sfaira, M. Taleb, B. Hammouti, M ; Ebn Touhami, S. Radi, Z. Rais, *J. Appl. Electrochem* (2010) 40: 1575-1582.

[8] A. El Ouafi, B. Hammouti, H. Oudda, S. Kertit, R. Touzani, A. Ramdani, *Anti-Corrosion Methods and Materials* (2002) 49(3) 199-204.

[9] M. Mobin and M. A. Khan, 2013, *Journal of Dispersion Science and Technology*, (2013).

[10] Y. Kaddouri, A. Takfaoui, F. Abrigach, M. El Azzouzi, A. Zarrouk, B. Hammouti, R. Touzani and H. Sdassi, *Journal of Materials and Environmental Sciences* (2017) 8 (3) 845-856.

[11] Gaussian 09, A. 02. Revision, M. J. Frisch, G. W. Trucks, H. B. Schlegel, G. E. Scuseria, M. A. Robb, J. R. Cheeseman, G. Scalmani, V. Barone, B. Mennucci, G. A. Petersson, H. Nakatsuji, M. Caricato, X. Li, H. P. Hratchian, A. F. Izmaylov, J. Bloino, G. Zheng, J. L. Sonnenberg, M. Hada, M. Ehara, K. Toyota, R. Fukuda, J. Hasegawa, M. Ishida, T. Nakajima, Y. Honda, O. Kitao, H. Nakai, T. Vreven, J. A. Montgomery, Jr., J. E. Peralta, F. Ogliaro, M. Bearpark, J. J. Heyd, E. Brothers, K. N. Kudin, V. N. Staroverov, R. Kobayashi, J. Normand, K. Raghavachari, A. Rendell, J. C. Burant, S. S. Iyengar, J. Tomasi, M. Cossi, N. Rega, J. M. Millam, M. Klene, J. E. Knox, J. B. Cross, V. Bakken, C. Adamo, J. Jaramillo, R. Gomperts, R. E. Stratmann, O. Yazyev, A. J. Austin, R. Cammi, C. Pomelli, J. W. Ochterski, R. L. Martin, K. Morokuma, V. G. Zakrzewski, G. A. Voth, P. Salvador, J. J. Dannenberg, S. Dapprich, A. D. Daniels, O. Farkas, J. B. Foresman, J. V. Ortiz, J. Cioslowski, and D. J. Fox, Gaussian, Inc., Wallingford CT, 2009.

[12] Touzani R., Ramdani A., Ben-Hadda T., El Kadiri S., Maury O., Le Bozec H., Diwneuf P.H., *synth. Commun.*, 31 (9) (2001)1315-1321

[13] I.A. Ammar, F.M. El Khorafi, Werkst. und Korros. 24 (1973) 702

[14] O. Benali, L. Larabi, B. Tabti, Y. Harek, Anti-Corros Met Mat., 52 (2005) 280-285.

[15] O. Benali, O. Mokhtar, Arab. J. Chem., 4 (2011) 443-448

[16] N.O. Eddy , E.E. Ebenso Afri J of Pure & Appl Chem 2(6) (2008) 1

[17] O. Radovici, Proc. 7 th European Symposium on Corrosion Inhibitors, Ann. Univ. Ferrara, Italy, (1990) p. 330

[18] E.E. Oguzie, V.O. Njoku, C.K. Enenebeaku, C.O. Akalezi, C. Obi, Corros. Sci. 50 (2008) 3480-3486.

[19] H. M. F. Freundlich, Over the adsorption in solution, j. Phys. Chem. 57 (1906) 385-471

[20] D.Landolt; Corrosion et Chimie de Surface des Métaux, 1st Edn, Alden Press, Oxford (1993) 495

[21] A. N. Frumkin, Progress in Surface Science, 8 (1977) 1-2

[22] S. O. Adejo, M. M. Ekwenchi, IOSR J. of Appli. Chem, (2014) 66-71

[23] I. B. Obot, N. O. Obi-Egbedi and S. A. Umoren, 2009, Inter. J. of Electrochem. Sci., 4, 863-877

[24] E. Mc cafferty, Corrosion Control by coating, Science Press, Princeton (1979)

[25] V.S. Sastri, J.R. Perumareddi, Corrosion, 53 (1997) 617

[26] K. Fukui, T. Yonezawa, H. Shingu, J. Chem. Phys., 20 (1952) 722